Hindawi
Shock and Vibration
Volume 2023, Article ID 2504170, 15 pages
https://doi.org/10.1155/2023/2504170

Research Article

Nonlinear Vibration Feature Recognition Method for Reciprocating Compressor Cylinder Based on VMD-Multifractal Spectrum

Fengxia Lyu, Caiqian Xie, Fengfeng Bie, Xinting Miao, Yifan Wu, and Ying Zhang

School of Mechanical Engineering and Rail Transit, Changzhou University, Changzhou 213016, Jiangsu, China

Correspondence should be addressed to Fengfeng Bie; bieff@cczu.edu.cn

Received 17 October 2022; Revised 2 January 2023; Accepted 3 January 2023; Published 17 January 2023

Academic Editor: Erkan Oterkus

The failure probability of piston ring abrasion occupies the forefront in reciprocating compressor cylinder assembly. Due to the reciprocating friction between the piston ring and cylinder liner, the local vibration signal contains typical nonstationary characteristics with a seriously overlapped frequency band of impact signals, while the different featured signals are coupled with each other. Therefore, the identification of cylinder friction and abrasion fault modes has always been a hot and difficult problem in fault diagnosis of reciprocating compressors. In order to monitor the friction and abrasion between low linear speed nonmetallic piston ring and cylinder liner of reciprocating compressor in refinery and provide a theoretical basis for preventive maintenance, an analysis method based on VMD-multifractal spectrum was presented in this paper. First, the feasibility of the proposed method was proven based on the cylinder vibration experiment of a reciprocating compressor in the laboratory. Then, an in-service reciprocating compressor in a refinery was taken as the research object, from which the cylinder friction vibration signals were processed by using variational mode decomposition to obtain a band-limited intrinsic mode function (BLIMF). Multifractal detrended fluctuation analysis is employed in the final abrasion pattern identification. The results show that the proposed method based on VMD-multifractal spectrum analysis can effectively obtain the abrasion state of a piston ring, which can avoid blind overhaul or provide the basis for preventive maintenance and a practicable engineering route for the study of the piston ring abrasion degree.

1. Introduction

As an important fluid conveying machine in the petrochemical industry, the common faults of the reciprocating compressor include valve failure, packing leakage, piston parts wear, big and small end bearing shells, crosshead pin fractures, etc., among which unplanned downtime caused by piston ring wear and fracture accounts for 10% of the total faults. Therefore, it is very important to study the wear monitoring of piston rings.

Comparing with traditional wear monitoring methods, including the cylinder pressure monitoring method and the oil monitoring method, the analysis method for vibration monitoring is the most practicable [1]. Compared with acoustic and thermal imaging, vibration monitoring also has some advantages. Vibration analysis, usually an online technique, has a relatively high efficiency in the data acquisition process, which can find problems at an early stage of failure. Although acoustic-based fault diagnosis is easier to install, the selection of the installation location is particularly crucial, and the selection of the measuring point location relies on experience, while the multichannel acquisition and manual or machine screening are additionally needed. Thermal imaging technology can quickly locate equipment components with large temperature changes when a fault occurs, usually for transformers, motors, etc. However, the precise fault diagnosis on the typical moving parts of the machinery system takes more time, which is not ideal as required. The frictional vibration of the piston ring and cylinder

liner contains a lot of information reflecting the tribological characteristics and friction state of the system [2]. Some researchers have developed vibration-based wear monitoring for life prediction [3]. However, the vibration signals collected directly are mixed with other mode signals of a reciprocating compressor, which are coupled with each other. The actual operating status of the reciprocating compressor could not be directly determined from the original friction vibration signals since the signal has nonstationary and non-linear characteristics [4]. The method of vibration analysis focuses on the frequency band energy and time-frequency domain characteristics of the vibration signal collected from the assembly surface. As for the typical study achievements, the wavelet Kullback–Leibler distance method [5], Hilbert's method of empirical mode decomposition [6], the local wave time-frequency method [7], etc., are presented gradually. However, for the nonlinear and nonstationary characteristics of the vibration, there are still some limitations in the classification of mode aliasing, preset wavelet analysis basis functions, or the number of intrinsic mode functions. Variational mode decomposition (VMD) was proposed as a new signal processing method by Dragomiretskiy and Zosso in 2014 [8], the core idea of which is the maxima problem with variational constraints. The band-limited intrinsic mode function (BLIMF) is obtained, which is different from EMD [9] and LMD [10]. The EMD and LMD methods used a cyclic sieving and stripping signal processing method. Therefore, the VMD method overcomes the mode aliasing problem and shows strong robustness in denoising [11–14]. In recent years, many scholars have applied it to signal analysis in related fields [15–17]. In view of the typical features of the nonlinear vibration of the reciprocating compressor cylinder block, including the impact of the air valve, the pulsation of the airflow, the friction vibration of the piston assembly, the mutual excitation and coupling between the moving parts, and so on [18], the basic VMD method could be applicable by presetting the scale K and constructing the variational framework, where the signal is decomposed into the variational model and the frequency center and bandwidth of the BLIMF components are determined by searching the optimal solution iteratively. This method could satisfy the condition of adaptive signal decomposition, and separates BLIMF components effectively by frequency domain segmentation, highlighting the local scale characteristics of data. Due to the periodicity and long-term unpredictability of the vibration signals of the reciprocating machine, the details of other reciprocating periods could be ignored when merely considering the discrete points of the vibration sequence. For the prediction of this kind of signal, it is necessary to describe the wave characteristics and invariable structure of a certain component of the signal at different time scales. Multifractal detrended fluctuation analysis [19] (MFDFA) is based on detrended fluctuation analysis proposed by Kantelhardt in 2002. The unsteady time series analysis method of DFA is a rapidly emerging nonlinear signal processing theory in recent years. It could divide a complex fractal into many small regions with different degrees of singularity, which is suitable for the self-similarity of complex systems analysis. Multifractal spectrum can describe the singularity of non-linear vibration signals well [20–22].

Aiming at the nonlinear vibration characteristic involved in the piston assembly at various wear statuses of the piston ring and cylinder liner, a method based on variational mode decomposition (VMD) and multifractal spectrum is presented through an experimental and engineering case study. This paper is organized in the following manner: Section 1 is the basic theory and research ideas; Section 2 is an experimental demonstration. The characteristic values of wear are obtained by processing the experimental signals with the proposed method. Section 3 is engineering verification, in which the proposed method is basically verified in an engineering application. The last part is the conclusion.

2. Description of Theoretical Background

2.1. Variational Mode Decomposition. In the VMD method, the intrinsic modal function (IMF) is expressed as follows:

$$uk(t) = Ak(t)\cos(\phi k(t)), \tag{1}$$

where $uk(t)$ is the IMF component from the vibration signal decomposition. $Ak(t)$ is the instantaneous amplitude. $\phi k(t)$ is an instantaneous phase. $\omega(t)$ is the derivative of $\phi k(t)$, which is the instantaneous frequency decomposition process and the solution process for variational problems.

If each modal component has the limited bandwidth of different center frequencies, the center frequency and bandwidth are continuously updated iteratively during the decomposition process, and the input signal F is decomposed into K discrete subsignals to minimize the estimated sum of the bandwidths of each subsignal. The variational process is specifically constructed as follows: an analytic signal of u_k is first obtained from the unilateral spectrum by Hilbert transformation, and then a central frequency index is added to obtain the corresponding base band. The square of the demodulation signal gradient L^2 is calculated, and the bandwidth of each subsignal is estimated. The constrained variational problem becomes

$$\begin{aligned} &\min_{\{u_k\},\{\omega_k\}} \left\{ \sum_k \left\| \partial_t \left[\left(\delta(t) + \frac{j}{\pi t} \right) * u_k(t) \right] e^{-j\omega_k t} \right\|_2^2 \right\} \\ &\text{S.t.} \sum_k u_k = f, \end{aligned} \tag{2}$$

where $\{u_k\} = \{u_1, \cdots, u_k\}$ represents K IMF components obtained by decomposition and $\{\omega_k\} = \{\omega_1, \cdots, \omega_k\}$ is the center frequency of each component obtained by decomposition.

Equilibrium constraint parameter α and Lagrange multiplication operator $\lambda(t)$ are used to solve the constructed constraint variational problem, so that the variational problem is no longer limited by constraint conditions, and the augmented Lagrange is introduced L as follows:

$$L\left(\{u_k\},\{\omega_k\},\lambda=\alpha\sum_k\left\|\partial_t\left[\left(\delta(t)+\frac{j}{\pi t}\right)*u_k(t)\right]e^{-jw_kt}\right\|_2^2+\left\|f(t)-\sum_k u_k(t)\right\|_2^2+\langle\lambda(t),f(t)-\sum_k u_k(t)\rangle. \tag{3}$$

The "saddle point" problem is solved by using the multiplier alternating direction algorithm. The components and frequencies are updated constantly. Finally, the "saddle point" of the unconstrained model is obtained, which is the optimal solution to the original problem. All component solutions are

$$\widehat{u}_k^{n+1}(w)=\frac{\widehat{f}(\omega)-\sum_{i\neq k}\widehat{u}_i(\omega)+(\widehat{\lambda}(\omega)/2)}{1+2\alpha(\omega-\omega_k)^2}, \tag{4}$$

where $\widehat{u}_k^{n+1}(w)$, $\widehat{f}(\omega)$, and $\widehat{\lambda}(\omega)$, respectively, represent the Fourier transforms of $\mu_k^{n+1}(\omega)$, $f(\omega)$, $\lambda(\omega)$. Meanwhile, the updated modal center frequency is expressed as follows:

$$\omega_k^{n+1}=\frac{\int_0^\infty\omega|\mu_k(\omega)|^2d\omega}{\int_0^\infty|\mu_k(\omega)|^2d\omega}. \tag{5}$$

VMD algorithm flow is as follows:

(1) Initialize: $\{u_k^1\},\{\omega_k^1\},\lambda^1$, N.

(2) $N=N+1$, execute the loop program.

(3) From $K=1$: the number of preset modes K, update $\{u_k\},\{\omega_k\}$.

(4) Update $\lambda^{n+1}=\lambda^n+\tau(f-\sum_k\widehat{u}_k^{n+1}(w))$.

(5) Repeat steps 3 and 4 until the iteration termination condition is satisfied as follows:

$$\sum_k\left\|u_k^{n+1}-u_k^n\right\|_2^2\left\|u_k^n\right\|_2^2<\varepsilon. \tag{6}$$

2.2. Theory and Algorithm of Multifractal Detrended Wave Analysis. The multifractal detrended wave analysis method can accurately calculate the multifractal spectrum of vibration signals. The feature of multifractal spectrum is more sensitive to the change of vibration signal, MFDFA algorithm step [19] is as follows:

(1) For the time series $\{x_i\}(i=1,2\ldots,n)$, calculate the deviation sequence $Y(i)$.

$$Y(i)=\sum_{k=1}^{i}(x_i-\overline{x})(i=1,2\ldots,n), \tag{7}$$

$\overline{x}$ is the average value of $\{x_i\}$.

(2) Divide $Y(i)$ into a N_s subinterval whose length is equal to s. Also, the subinterval is continuous and nonoverlapping.

$$N_s=\text{int}\left(\frac{N}{s}\right). \tag{8}$$

When N cannot divide s exactly, to ensure the integrity of information, the data are reversely repeated in this segmentation process to obtain 2 N_s subintervals.

(3) The mean square error was calculated, and the k-order multiform fitting was carried out by the following least squares method:

When the interval is $(t=1,2,3,\ldots,N_s)$, the mean square error is $F^2(s,t)$.

$$F^2(s,t)=\frac{1}{s}\left(\sum_{i=1}^{s}\{Y[(t-1)s+i]-y_t(i)\}^2. \tag{9}$$

When the interval is $(t=N_s+1,N_s+2,\ldots,2N_s)$, the mean square error is $F^2(s,t)$.

$$F^2(s,t)=\frac{1}{s}\left(\sum_{i=1}^{s}\{Y[N-(t-1)s+i]-y_t(i)\}^2. \tag{10}$$

(4) Calculate the q-order wave function $F_q(s)$.

$$F_q(s)=\left\{\frac{1}{2N}\sum_{t=1}^{2N_s}\left[F^2(s,t)\right]^{(q/2)}\right\}^{(1/q)}. \tag{11}$$

When $q>0$, it reflects the big fluctuation trend of the time series; otherwise, it represents the small fluctuation trend of the time series.

(5) Calculate the power relation between the logarithmic function of $F_q(s)$ to order and the time scale s.

$F_q(s)\sim s^{h(q)}$. $h(q)$ is the generalized Hurst index.

(6) Analyze the logarithmic function of $F_q(s)$ with respect to scale to obtain the wave function $\tau(q)$.

$$\tau(q)=qh(q)-1. \tag{12}$$

(7) Calculate the global singularity of the multifractal and the dimension of the multifractal set as follows:

$$\begin{aligned}\alpha&=\frac{\mathrm{d}\tau(q)}{\mathrm{d}q}\\&=h(q)+qh\dot{(}q),\\f(\alpha)&=q\alpha-\tau(q)\\&=q[\alpha-h(q)]+1.\end{aligned} \tag{13}$$

2.3. Diagnostic Model and Research Ideas. This paper constructs a fault diagnosis model based on VMD-MFDFA for the fault diagnosis of a reciprocating compressor cylinder block. The block diagram of the overall review of the research is shown in Figure 1.

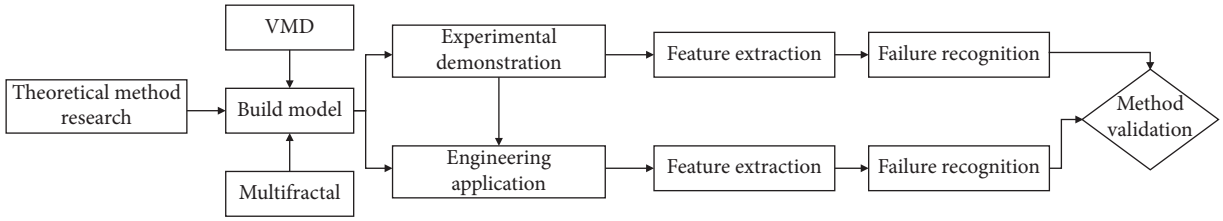

Figure 1: Research flow block diagram.

The specific steps are as follows:

(1) Set up a test platform to collect nonlinear vibration signals of the piston ring under normal and wear conditions.

(2) Variational mode decomposition (VMD) was used to process the signal. After the decomposition, the vibration signal of the air valve was removed and the signal was reconstructed.

(3) Multifractal processing was performed on each group of signals. Extract the characteristic value of wear, such as the Hurst index.

(4) Carry out an engineering application to verify the feasibility of the method.

The technical route is shown in Figure 2.

3. Experimental Demonstration

3.1. Experimental Platform. The experiment was conducted on a SpectraQuest mechanical fault simulation test bench, as shown in Figure 3. The compressor was a vertical, single cylinder compressor driven by a belt.

The structure of the test rig is shown in Figure 4. The structural dimensions of the equipment are listed in Table 1.

3.2. Data Collection. In order to accurately monitor the operation of the piston ring, the outside of the cylinder block where the piston reciprocates was selected as the vibration collection point [23]. The cylinder vibration data in the early fault and late period of compressor operation were collected, as shown in Figures 5(a) and 5(b).

Figure 5 shows the vibration time domain waveform of the compressor cylinder at the early and late stages. The overall signal is nonlinear and nonstationary. The vibration signal of the cylinder block includes the vibration and impact signal brought by the airflow when the valve is on and off. With the increasing wear of the piston assembly, the vibration amplitude of the late stage is lower than that of the early stage, but the waveform becomes more disorderly and irregular. Figure 6 shows the time-frequency spectrum of cylinder vibration. Since the piston ring of the compressor is self-sealing, the piston ring can be close to the sides of the cylinder liner and ring groove by means of the pressure difference on both sides (the upper and lower sides and the left and right sides), so the switch function of the air valve is still needed in the measurement process. The friction vibration signal of the piston component is drowned in other vibration signals, so the nonlinear vibration of the cylinder block cannot be studied only by analyzing this signal.

3.3. VMD. Variational mode decomposition was used to decompose the signal. The optimal component was confirmed by the central frequency observation method and the spectrum map. The solution parameter is $K = 2$. The bandwidth limit $\alpha = 1000$. Decompose it into two modal components. The early and end-stage VMD are shown in Figures 7–10.

According to the time-frequency image of the nonlinear vibration of a cylinder block shown in Figure 6, the frequency range of the gas impact caused by the switch of the air valve is about 1600 Hz to 1800 Hz. In addition, the friction vibration between the piston ring support ring and cylinder block at the cylinder block side is considered to be characterized by low frequency and amplitude. Therefore, BLIMF2 was selected as an effective signal to remove the influence of the gas valve and carry out reconstruction. The reconstructed signal is shown in Figures 11(a) and 11(b).

3.4. Multifractal Detrended Wave Analysis of Cylinder Block Nonlinear Vibration. A multifractal analysis algorithm was used to analyze the reconstructed signal. The signal had sixteen reciprocating operation cycles. By setting different scales S and different orders q, the signals were grouped and the overall wave function was calculated. The scales S were 16, 32, 64, 128, 256, 512, and 1024. When q was 2, local fluctuation and global fluctuation of early data were calculated respectively.

In Figure 12, the blue line represents local fluctuations. It could be observed that, in the same order, fluctuations at the small scale are more obvious than those at the large scale. Since there are more data at the large scale, there is less difference in fluctuations after averaging with each other. The red line represents global fluctuations at different scales, with smaller global fluctuations at smaller scales. By setting q differently, the fluctuation of the time series could be distinctively reflected.

Taking q in the following order: −5, −3, −1, 1, 3, and 5. The nonlinear vibration of the cylinder block at the early and late phases of operation is analyzed. The scale S of 16, 32, 64, 128, 256, 512, and 1024 were taken as the study objects, respectively. It could be found that different order is obviously different from the q-order wave function through Figures 13(a) and 13(b). The reason is that the small scale does not span a reciprocating motion period, while at the

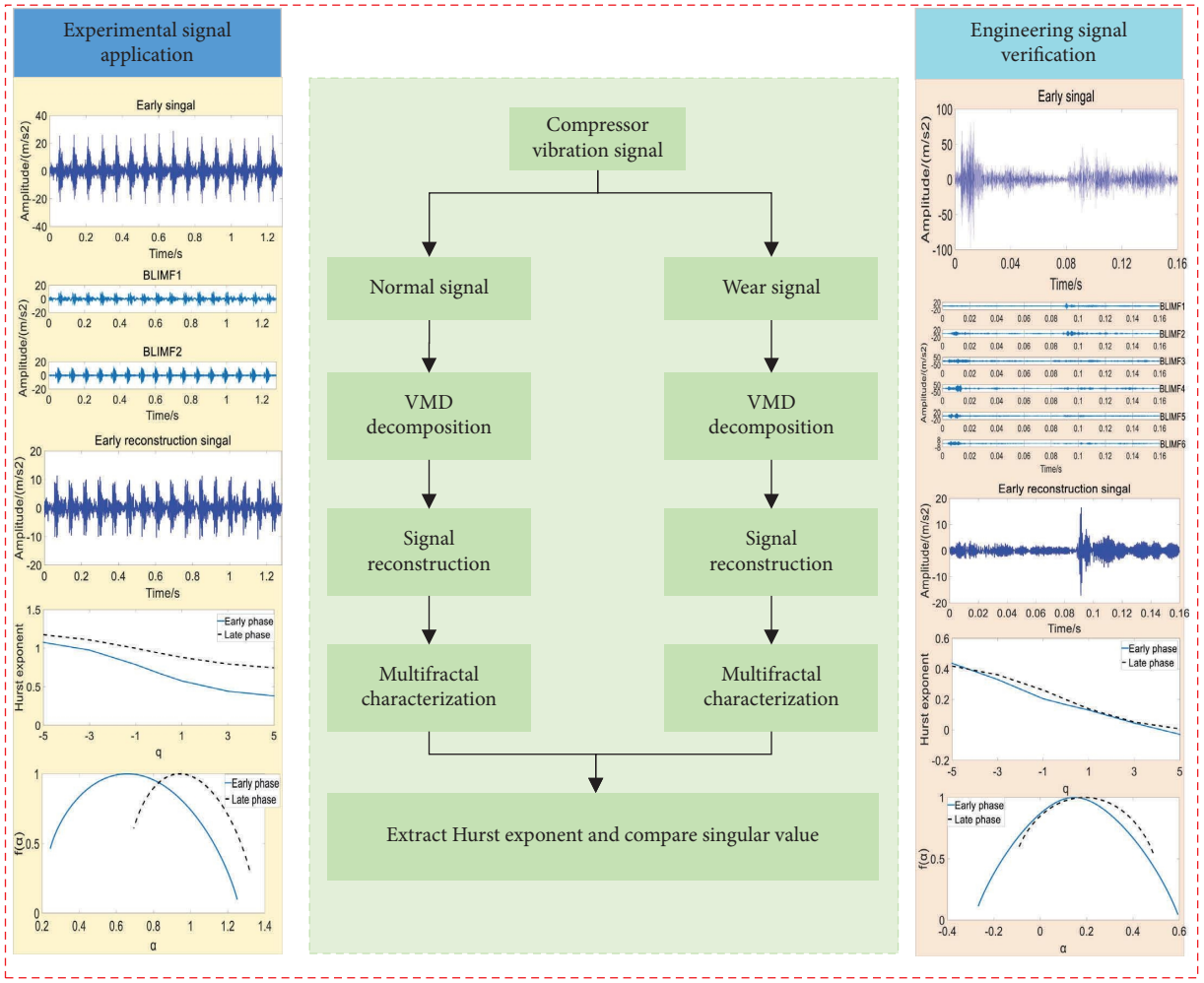

Figure 2: Technical route.

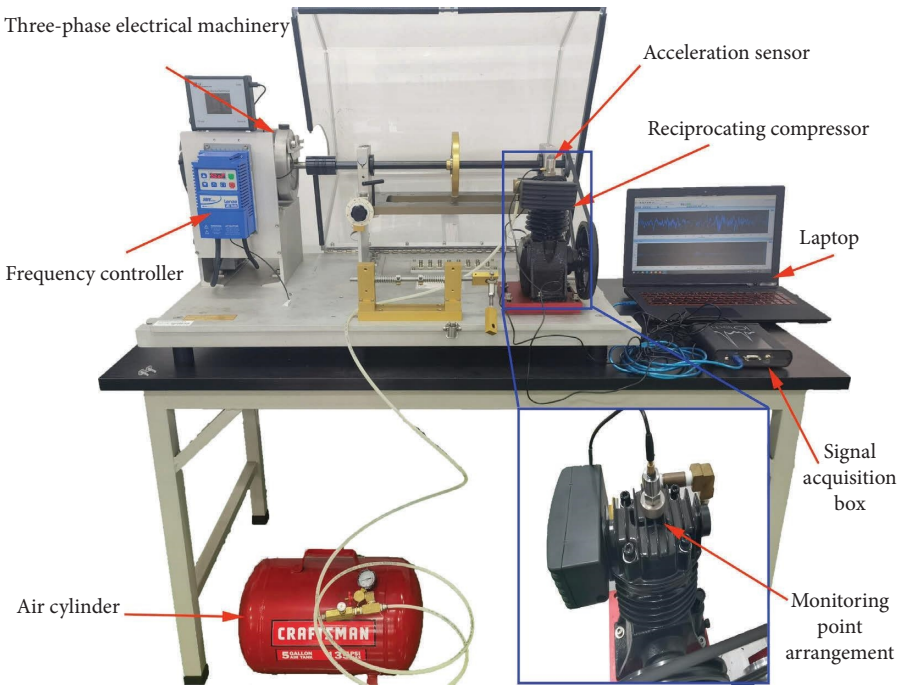

Figure 3: Experimental bench and test system.

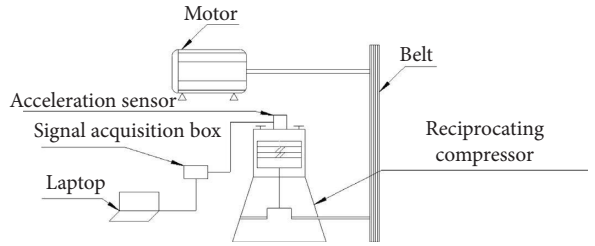

Figure 4: The structure of the test rig.

Table 1: Experimental system and structure size parameter table.

Inner diameter of cylinder block	5.08 cm
Compressor flow	0.07 m^3/s
Operation period	0.078 s
Piston ring radial early thickness	3 mm
Lubrication form	Oil free
Acceleration sensor	DH1A110E
Sampling frequency	12800 Hz
Stroke	3.81 cm
Outlet pressure	0.8 MPa
Piston ring material	PTFE
Piston ring radial end thickness	2.8 mm
Motor speed	1420 r/min
Sensitivity	5.088 mV/(m/s^2)
Sampling time	1.28 s

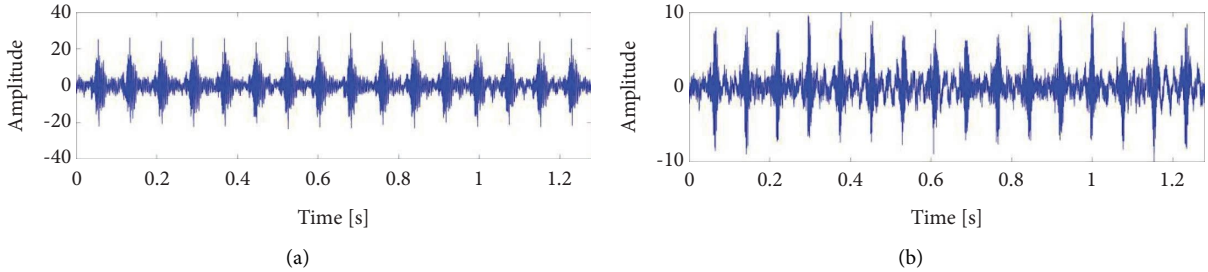

Figure 5: Time-frequency diagram of vibration signals. (a) Early stage. (b) Late stage.

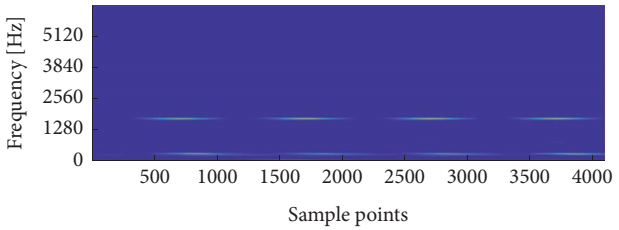

Figure 6: Time domain waveform of a vibration signal.

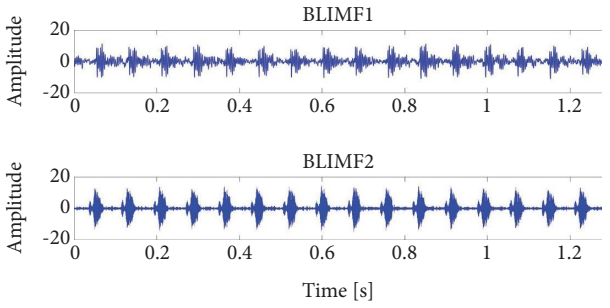

Figure 7: Two groups of BLIMF components of early VMD.

large scale, the wave functions of all orders tend to keep the same.

The Hurst exponent defines the growth rate of fluctuation of a nonlinear vibration signal at different sample scales, which is the slope Hq of the regression line. If $Hq > 1$, it indicates that the time series has a long-term dependence. When Hq is between 0.5 and 1, it indicates that the time series has a long correlation structure and the vibration trend is more stable. Hq is between 0 and 0.5, indicating that

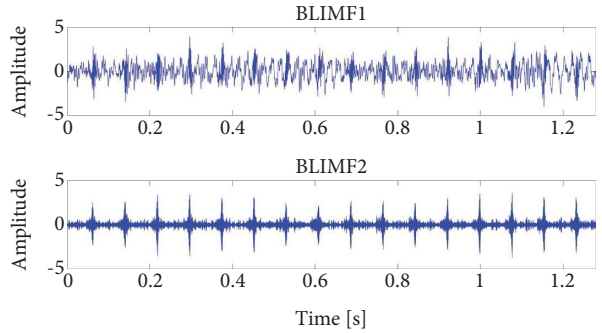

Figure 8: Two groups of BLIMF components of end-stage VMD.

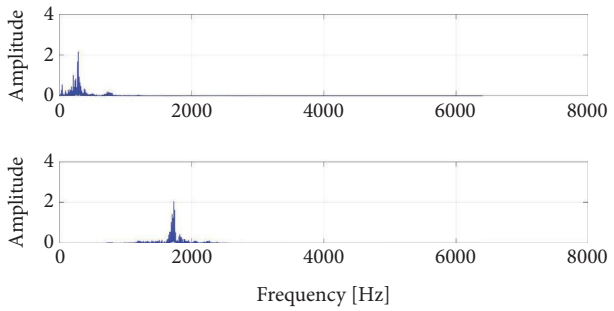

Figure 9: Fourier transforms of two early BLIMF components.

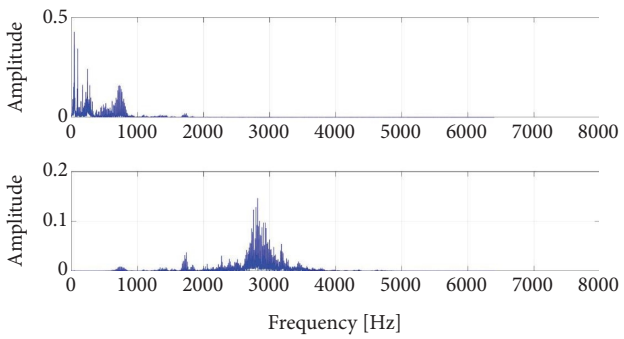

Figure 10: Fourier transforms of two BLIMF components in the terminal stage.

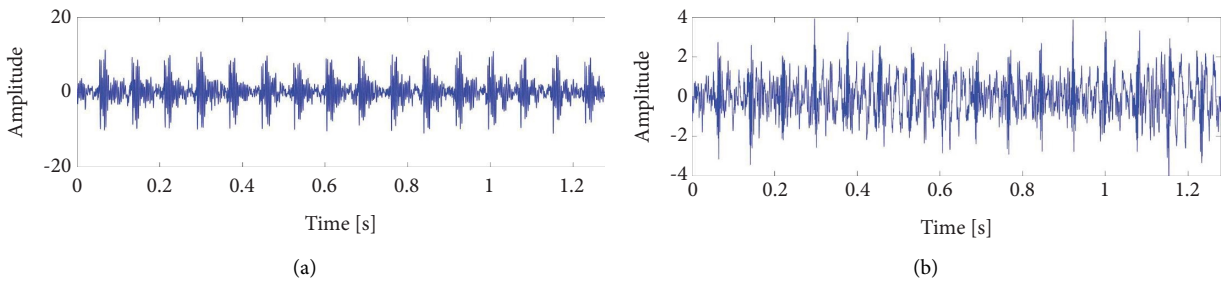

Figure 11: Reconstructed signal diagram. (a) An early reconstruction signal. (b) A late reconstruction signal.

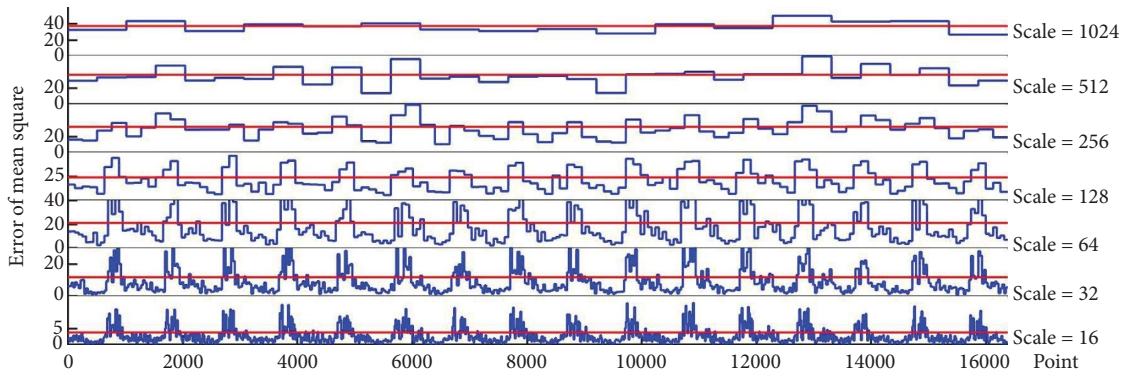

Figure 12: Mean square error at different scales.

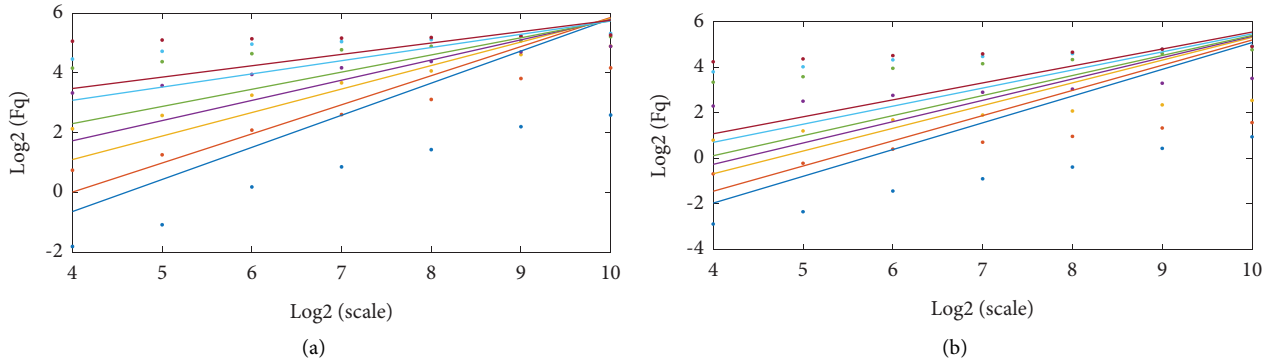

Figure 13: Logarithmic regression line of wave function and scale. (a) Early function. (b) Late function.

the time series has an inverse correlation structure. Based on Figures 13 and 14, multifractal characteristics could be observed in the nonlinear vibration of a cylinder block. Combined with Table 2, the Hurst index of the early phase is less than the last phase, which indicates that the piston ring, the supporting ring, and the cylinder block in the case of normal oil injection, with the thinning of the thickness, the constraint between each other becomes smaller, the working face is much smoother, and the vibration of mutual excitation is reduced, while the frictional vibration goes stable.

Combined with Figure 15 and Table 3, for the order $q > 0$, the scaling exponent of the late phase is larger than the early phase. For the order $q < 0$, the late value is smaller than the early value.

Table 4 illustrates the multifractal spectrum parameters of nonlinear vibration signals of the cylinder block, in which $\alpha_{\max}$ is the maximum value and $\alpha_{\min}$ is the minimum value of the singular index. $\delta_\alpha = \alpha_{\max} - \alpha_{\min}$. $F(\alpha)_{\max}$ is the maximum value of the fractal dimension function of the singular exponent of the multifractal set. $F(\alpha)_{\min}$ is the minimum value of the fractal dimension function of the singular exponent of the multifractal set. $\delta_F = F(\alpha)_{\max} - F(\alpha)_{\min}$. $\alpha_{f\max}$ is the singular index after the fractal function reaches the maximum value. The width of the multifractal spectrum is 1.005 at the initial stage of the nonlinear vibration of a cylinder block and 0.406 at the end. δ_α shows a gradually smaller trend. From the physical significance of δ_α

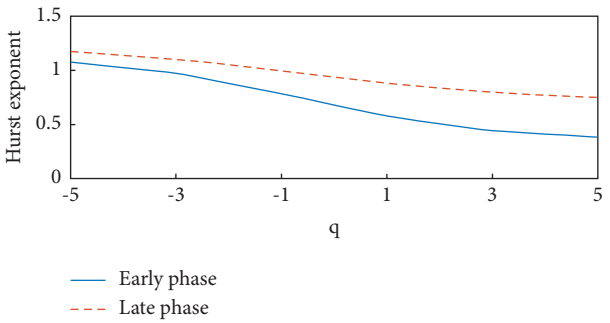

Figure 14: Hurst exponents at the early and late phases.

Table 2: Hurst exponent of the nonlinear vibration signal of the cylinder block.

Hurst exponents	$q=-5$	$q=-3$	$q=-1$	$q=1$	$q=3$	$q=5$
Early phase	1.074	0.974	0.786	0.574	0.441	0.380
Late phase	1.174	1.106	0.998	0.880	0.794	0.744

in the late stage of piston ring operation, the amplitude distribution range of the vibration signal gets smaller. In the early stage of compressor operation, the vibration fluctuation between the piston assembly and cylinder block is relatively violent, the signal energy is strong, and the

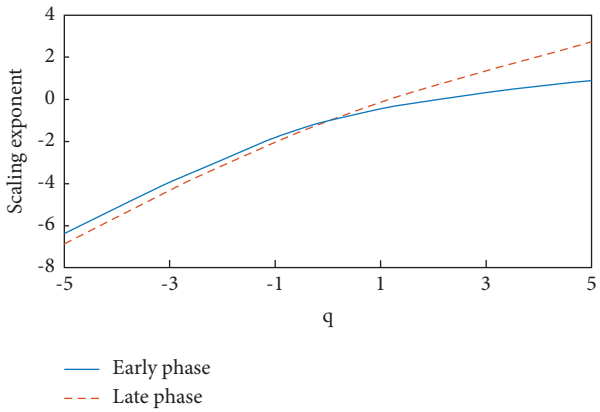

Figure 15: Early and late scaling exponent.

Table 3: Scale index of the nonlinear vibration signal of the cylinder block.

Index of the scales	$q=-5$	$q=-3$	$q=-1$	$q=1$	$q=3$	$q=5$
Early phase	6.373	3.922	1.786	0.425	0.325	0.902
Late phase	6.873	4.320	1.998	0.119	1.382	2.722

multifractal characteristics are stronger. The early value $\alpha_{\min}$ is less than the late value, which reflects that the signal changes rapidly and the vibration signal fluctuates greatly. The early stage δ_F is 0.898 and the late stage δ_F is 0.691, which shows a decreasing trend of δ_F, i.e., the larger the δ_α, the larger the δ_F, the smaller the $\alpha_{f\max}$, the stronger the multifractal properties.

From the fractal spectrum shape, the early parabola has a wide distribution of zeros, and the extreme point is closer to the Y-axis. Compared with the early working conditions, the piston ring and support ring components will wear to different degrees, and the extreme point will shift to the right end.

In conclusion, MFDFA can fully reveal the multifractal characteristics of time series in nonlinear vibration and the multifractal spectrum. Figure 16 can describe the dynamic behavior of a time series. The shape, spectrum width, extreme point, and other characteristic parameters of a multifractal spectrum are sensitive to changes in system state and can be used as characteristic parameters to characterize the system state of a reciprocating compressor cylinder block.

4. Engineering Verification

4.1. Research Object. The test data came from the reciprocating compressor in service in a refinery. The engineering test is shown in Figure 17. The unit is a symmetrical balance type with four columns and three-stage compression. The unit innovatively adopts a new hydrogen and cycle hydrogen combined compressor, in which three cylinders are used for three-stage compression of new hydrogen and another cylinder is used to boost the pressure of cycle hydrogen. The system and construction parameters are shown in Tables 5 and 6, where the test data collected from the cycling cylinder is set as the object.

Table 4: Dimensions of multifractal global singular values and multifractal sets.

Spectrum parameters	$\alpha_{\max}$	$\alpha_{\min}$	δ_α	$F(\alpha)_{\max}$	$F(\alpha)_{\min}$	δ_F	$\alpha_{f\max}$
Early phase	1.250	0.244	1.005	1	0.1017	0.898	0.670
Late phase	1.179	0.772	0.406	1	0.3089	0.691	0.947

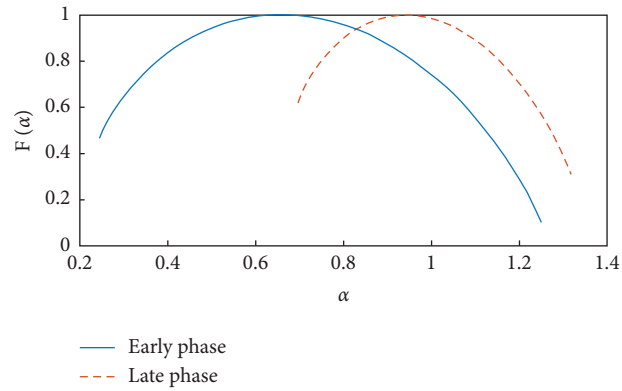

Figure 16: Multifractal spectrum.

4.2. Data Collection. The cylinder vibration data in the early and late period of compressor operation were collected with a sampling frequency of 25600 Hz and 4096 points, as shown in Figures 18(a) and 18(b).

4.3. VMD. The number of modes was confirmed by comparing the center frequencies of different K values. Bandwidth limit $\alpha=2000$. The following table shows the processing of end-stage data.

As can be observed from Table 7, when the number of modes is set to 7, components with similar center frequencies of 5671 Hz and 6518 Hz appear, and thus the K value is finally set at 6. Through VMD, the nonlinear vibration signal of a cylinder block can be effectively decomposed from a high-frequency to a low-frequency mode, and the phenomenon of mode aliasing can be restrained to a greater extent. In addition, the vibration of air valve excitation is effectively distinguished. The VMD of end-stage signals is shown in Figures 19 and 20.

From the time-frequency image of the nonlinear vibration of a cylinder block in Figure 21, the switching frequency segment of the air valve is about 3750 Hz to 7500 Hz. Therefore, BLIMF1 was selected as an effective signal to remove the influence of the gas valve and carry out reconstruction. The reconstructed signal is shown in Figures 22(a) and 22(b).

4.4. Multifractal Detrended Wave Analysis of Cylinder Block Nonlinear Vibration. Similarly, the scales S were 16, 32, 64,

Figure 17: Real-time vibration data acquisition of a reciprocating compressor.

Table 5: Dimensions and parameters of a refinery recovery machine.

Unit model	4HHE-VG-3-1
Compressor flow	26928 Nm^3/s
Outlet pressure	17 MPa
Medium	Circulating hydrogen
Outer dead center clearance	28.48 mm
Lubrication form	Oil lubrication
Lubricating oil name:	SHELL S1 B460
Stroke	323.85 mm
Inlet pressure	14 MPa
Piston ring material	Carbon-PTFE
Piston ring interface mode	45° oblique incision
Inner dead center clearance	1.57 mm
Cylinder size	171.4 mm
Motor speed	330 r/min

Table 6: Signal acquisition system.

Instrument name	BH550
Analysis frequency	100–20000 Hz
Analysis frequency	10000 Hz
Platform	WindowsCE
Frequency resolution	1/64 Hz
Analysis line number	1600

128, 256, 512, and 1024. When q was 2, the local fluctuation and the overall fluctuation of the final data were calculated, respectively, as shown in Figure 23.

Taking the order q as −5, −3, −1, 1, 3, and 5 individually, the logarithmic relationship between scale and $F_q(s)$ was calculated, as shown in Figures 24(a) and 24(b).

On a small scale, different orders has a great difference in the q-order wave function, which is more obvious in the early stage of piston ring operation. While on a relatively large scale, all order wave functions also tend to be consistent.

According to Figure 25, when the order $q > 0$, the late value is larger than the early value. Also, when the order is $q < 0$, the late value is also basically smaller than the early value.

It can be seen from Figure 26 that the nonlinear vibration of the cylinder block contains multifractal characteristics, while the Hurst index in the early stage is basically smaller than in the late stage, which is consistent with the experimental study. It can be considered that the Hurst index will increase at different orders at the end with the aggravation of piston ring wear.

Table 8 shows the multifractal spectrum parameters of the nonlinear vibration signals of the cylinder block, and the characteristics of the spectrum parameters are similar to the results of the experimental platform. According to the fractal spectrum (Figure 27), the early parabolic extreme point is closer to the Y-axis, and the extreme point also transforms to the right end of the parabola compared with the early conditions, and the zeros distance becomes narrower.

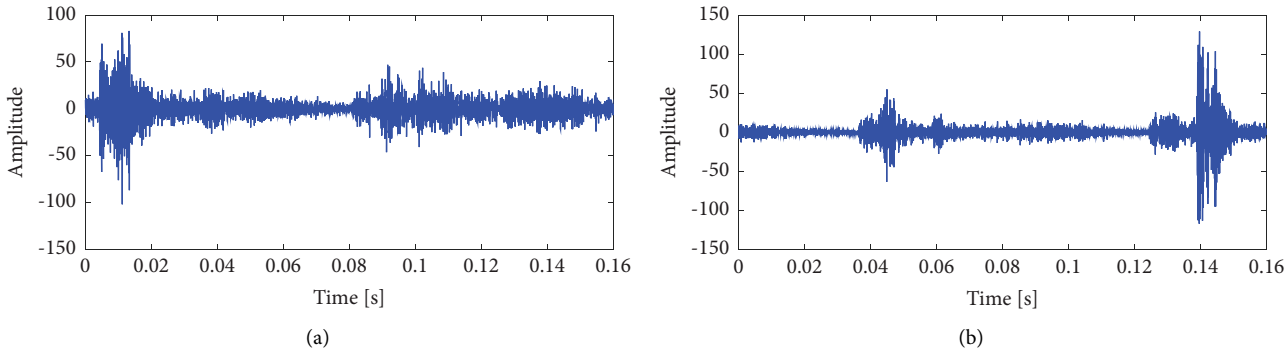

Figure 18: Time domain waveform of a vibration signal. (a) Early stage. (b) Late stage.

Table 7: Center frequencies under different K values.

K	Center frequency						
$K=2$	2355	5867					
$K=3$	2334	5294	6798				
$K=4$	1890	4440	5905	8024			
$K=5$	1749	3951	5569	6503	8782		
$K=6$	1637	3318	4991	5971	7817	9697	
$K=7$	1603	2982	4409	5671	6518	8073	9966

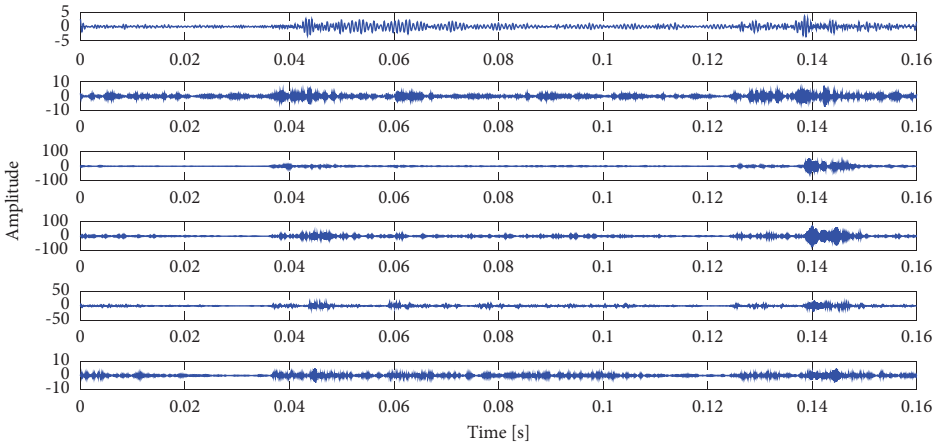

Figure 19: BLIMF components obtained by VMD.

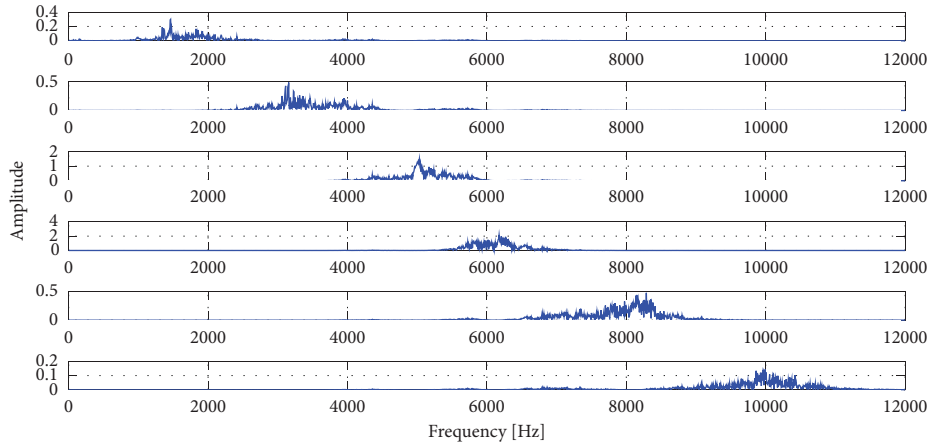

Figure 20: Spectrum of the BLIMF components.

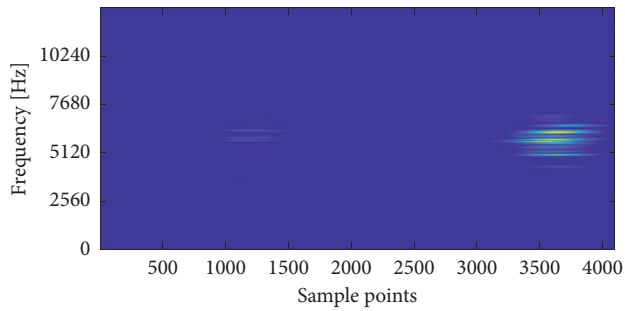

Figure 21: Time-frequency diagram of the cylinder vibration signal.

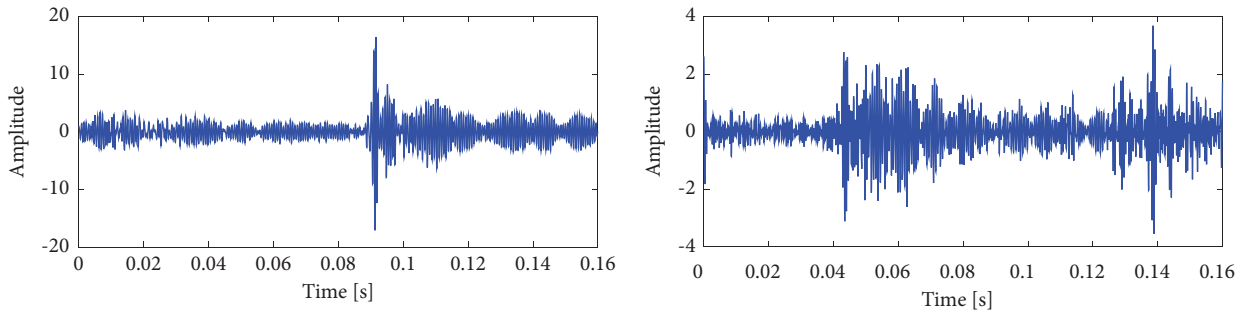

Figure 22: Reconstructed signal diagram. (a) An early reconstruction signal. (b) A late reconstruction signal.

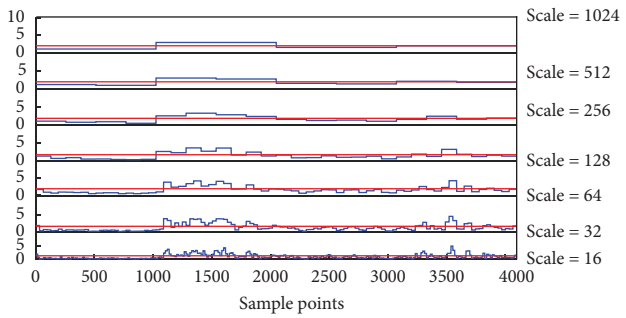

Figure 23: Wave at different scales.

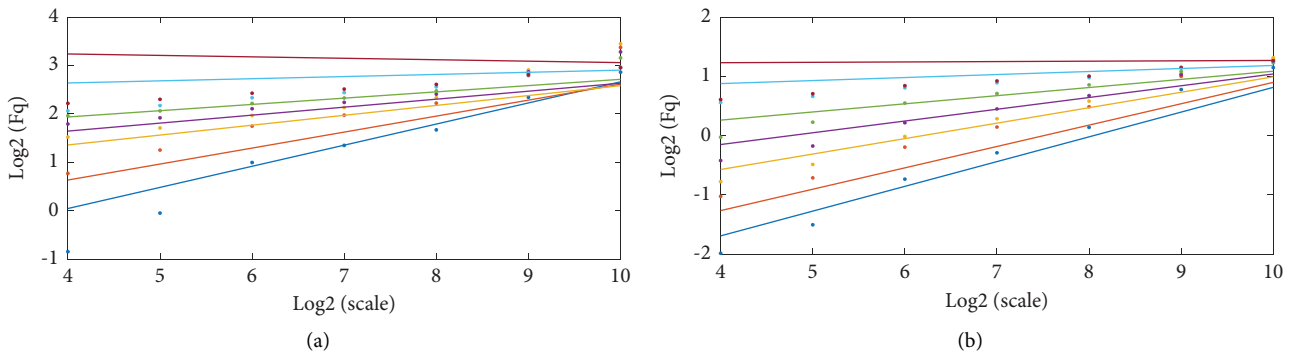

Figure 24: Logarithmic regression line of wave function and scale. (a) Early function. (b) Late function.

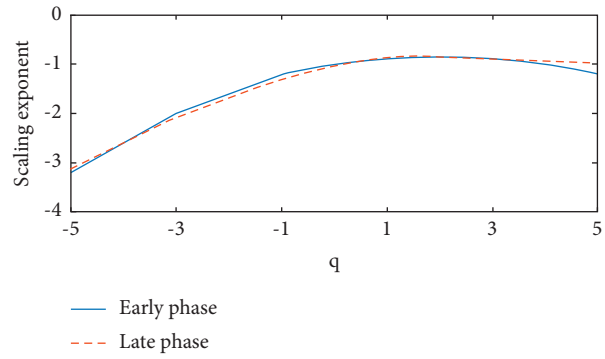

Figure 25: Early and late scaling exponents.

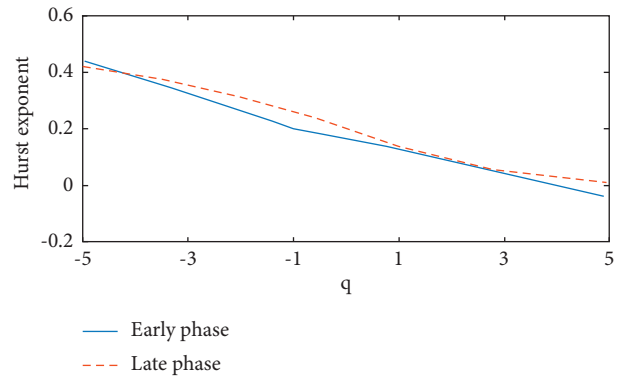

Figure 26: Hurst exponent of cylinder block nonlinear vibration.

Table 8: Dimensions of multifractal global singular values and multifractal sets.

Spectrum parameters	$\alpha_{\max}$	$\alpha_{\min}$	$\delta\alpha$	$F(\alpha)_{\max}$	$F(\alpha)_{\min}$	δF	$\alpha_{f\max}$
Early phase	0.628	0.169	0.798	1	0.0378	0.962	0.168
Late phase	0.519	0.074	0.593	1	0.4947	0.505	0.204

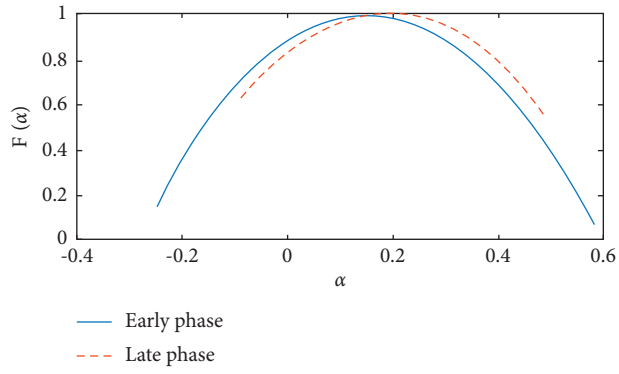

Figure 27: Multifractal spectrum.

Figure 28 shows the comparison between the old piston ring and the new piston ring during unit maintenance. The radial thickness of the new piston ring is 12.8 mm, while the radial thickness of the old piston ring is uneven, with an average of 9.12 mm and a local value of 6.29 mm. To sum up, their multifractal spectrum contains the abovementioned corresponding characteristics as the piston ring and support ring components in different wearing statuses.

Experiments and engineering have shown that the Hurst index of the early phase is less than the late phase. The shape,

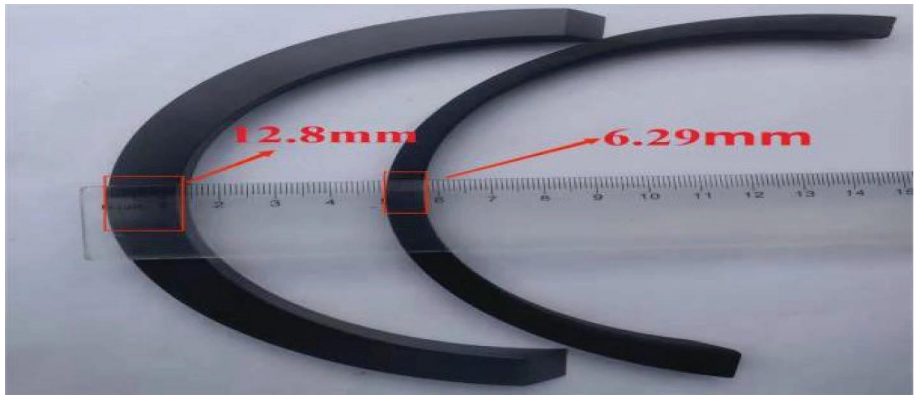

Figure 28: Comparison of early and late piston ring thicknesses.

spectrum width $\delta\alpha$, extreme point $\alpha_{f\max}$, and other characteristic parameters of a multifractal spectrum are sensitive to changes in system state and can be used as characteristic parameters to characterize the system state of a reciprocating compressor cylinder block. As the wear and tear intensifies, δ_α, δ_F becomes smaller and $\alpha_{f\max}$ becomes larger.

5. Conclusion

In this paper, the compressor platform was built, and the VMD-multifractal spectrum method was used in the wear experiment. A method based on VMD variational mode decomposition for nonlinear vibration analysis of cylinder blocks is proposed, which can effectively extract friction vibration signals from piston assemblies and cylinder blocks:

(1) With the proposed method, the nonlinear vibration of the cylinder block is processed, and the wear state of the piston assembly can be preliminarily figured out, which could provide valuable advice for preventive maintenance and replacement of the piston assembly.

(2) With the multifractal method, the wave characteristics of the nonlinear vibration of the cylinder block could be effectively figured out, combined with the general increasing trend of the Hurst index, which shows that the nonlinear vibration of the cylinder block of a reciprocating compressor is persistent.

(3) The experimental results show that the VMD-multifractal spectrum can qualitatively analyze the wear condition of the cylinder piston assembly. It is found that the width of the multifractal spectrum decreases with the wearing process, and the nonlinearity of the cylinder vibration signal can be characterized by the multifractal spectrum and the corresponding indicators.

However, the potential impact of other compressor components on non-linear cylinder vibration, such as spindle shingle wear, small and large head shingle wear, cross-head loosening, piston rod steering impact, etc., should be carefully considered in future research. The influence of these factors on the non-linear impact of the cylinder block and the fault diagnosis of the reciprocating compressor may be solved in future research. In addition, for the proposed VMD-multifractal spectrum method used in other types of equipment fault diagnosis, the extraction method for the typical fault features will also be the focus of future research.

Data Availability

The data used to support the findings of this study are available from the corresponding author upon request.

Conflicts of Interest

The authors declare that they have no conflicts of interest.

Acknowledgments

The study was supported by the project of National Natural Science Foundation of China (Grant no. 52105141), Natural Science Research Project of Universities in Jiangsu Provincial (Grant nos. 19KJA430004 and 21KJB460002) and Jiangsu Key Laboratory of Green Process Equipment.

References

[1] T. Liu and Z. Wu, "A vibration analysis based on wavelet entropy method of a Scroll Compressor," *Entropy*, vol. 17, no. 12, pp. 7076–7086, 2015.

[2] S. R. Ge and H. Zhu, "Quantitative research methods for complex tribological systems and their problems," *Tribology*, vol. 22, no. 5, pp. 405–408, 2002.

[3] K. Feng, J. C. Ji, Q. Ni, and M. Beer, "A review of vibration-based gear wear monitoring and prediction techniques," *Mechanical Systems and Signal Processing*, vol. 182, Article ID 109605, 2023.

[4] J. M. Li, H. J. Wei, L. D. Wei, D. P. Zhou, and Y. Qiu, "Extraction of frictional vibration features with multifractal detrended fluctuation analysis and friction state recognition," *Symmetry*, vol. 12, no. 2, p. 272, 2020.

[5] P. Zhou, H. Li, and D. Clelland, "Pattern recognition on diesel engine working conditions by wavelet kullback-leibler

distance method," *Part C: Journal of Mechanical Engineering Science*, vol. 219, no. 9, pp. 879–887, 2005.

[6] G. H. Jiang, K. Zhao, Z. Wang, Z. Yang, and X. Zeng, "Fault diagnosis of diesel cylinder liner wear based on hilbert transform based on EMD," *Journal of Shanghai Maritime University*, vol. 35, no. 3, pp. 80–84, 2014.

[7] C. M. Huang, Y. Liao, Q. Li, H. Yu, J. Liao, and C. C. Chen, "Assessment of health of friction pair in sliding bearing using vibration sensor and continuous wavelet transform time-frequency images," *Sensors and Materials*, vol. 32, no. 10, pp. 3531–3542, 2020.

[8] K. Dragomiretskiy and D. Zosso, "Variational mode decomposition," *IEEE Transactions on Signal Processing*, vol. 62, no. 3, pp. 531–544, 2014.

[9] N. E. Huang, Z. Shen, S. R. Long et al., "The empirical mode decomposition and the Hilbert spectrum for nonlinear and non-stationary time series analysis," *Series A: Mathematical, Physical and Engineering Sciences*, vol. 454, pp. 903–995, 1998.

[10] J. S. Smith, "The local mean decomposition and its application to EEG perception data," *Journal of The Royal Society Interface*, vol. 2, no. 5, pp. 443–454, 2005.

[11] X. Bi, S. Cao, and D. Zhang, "A variety of engine faults detection based on optimized variational mode decomposition-robust independent component analysis and fuzzy c-mean clustering," *IEEE Access*, vol. 7, pp. 27756–27768, 2019.

[12] F. F. Bie, K. V. Horoshenkov, J. Qian, and J. F. Pei, "An approach for the impact feature extraction method based on improved modal decomposition and singular value analysis," *Journal of Vibration and Control*, vol. 25, no. 5, pp. 1096–1108, 2019.

[13] Q. Ni, J. C. Ji, K. Feng, and B. Halkon, "A fault information-guided variational mode decomposition (FIVMD) method for rolling element bearings diagnosis," *Mechanical Systems and Signal Processing*, vol. 164, Article ID 108216, 2022.

[14] A. Kumar, C. P. Gandhi, G. Vashishtha et al., "VMD based trigonometric entropy measure: a simple and effective tool for dynamic degradation monitoring of rolling element bearing," *Measurement Science and Technology*, vol. 33, no. 1, Article ID 014005, 2021.

[15] C. Wang, H. Li, G. Huang, and J. Ou, "Early fault diagnosis for planetary gearbox based on adaptive parameter optimized vmd and singular kurtosis difference spectrum," *IEEE Access*, vol. 7, pp. 31501–31516, 2019.

[16] C. Zhang, Y. B. Zhang, C. Hu, Z. Liu, L. Cheng, and Y. Zhou, "A novel intelligent fault diagnosis method based on variational mode decomposition and ensemble deep belief network," *IEEE Access*, vol. 8, pp. 36293–36312, 2020.

[17] X. Y. Zhou, Y. B. Li, L. Jiang, and L. Zhou, "Fault feature extraction for rolling bearings based on parameter-adaptive variational mode decomposition and multi-point optimal minimum entropy deconvolution," *Measurement*, vol. 173, Article ID 108469, 2021.

[18] Z. N. Jiang, M. Y. Jin, B. Ma, and J. Zhang, "Research and application of intelligent diagnosis expert system for reciprocating compressor," *Fluid Machinery*, vol. 42, no. 4, pp. 37–41+27, 2014.

[19] J. W. Kantelhardt, S. A. Zschiegner, E. Koscielny-Bunde, S. Havlin, A. Bunde, and H. E. Stanley, "Multifractal detrended fluctuation analysis of nonstationary time series," *Physica A: Statistical Mechanics and Its Applications*, vol. 316, no. 1–4, pp. 87–114, 2002.

[20] Y. Feng, B. Lu, and D. Zhang, "Multifractal manifold for rotating machinery fault diagnosis based on detrended fluctuation analysis," *Journal of Vibroengineering*, vol. 18, no. 8, pp. 5153–5173, 2016.

[21] G. Y. Chen, C. F. Yan, J. D. Meng, Z. G. Wang, and L. X. Wu, "Health condition monitoring of bearings based on multifractal spectrum feature with modified empirical mode decomposition-multifractal detrended fluctuation analysis," *Structural Health Monitoring*, vol. 21, no. 6, pp. 2618–2640, Article ID 14759217211065991, 2022.

[22] G. B. Li, Y. Huang, Y. Lin, and X. Pan, "Multifractal analysis of frictional vibration in the running-in process," *Tribology Transactions*, vol. 56, no. 2, pp. 284–289, 2013.

[23] Y. Zhang, Y. C. Zhou, and Z. P. Zhang, "Study on diagnosing piston ring failure by body surface vibration signal," *Journal of Vibration Engineering*, vol. 4, pp. 48–53, 1997.